IEEE Robotics and Automation Letters, 2019

Degenerate Motion Analysis for Aided INS with Online Spatial and Temporal Sensor Calibration

康 腾

2019.09.22

CONTENT OF REPORT

- **Part 1. VIO 外参 / 时间差在线标定**
- **Part 2. 退化运动的可观性分析**
- **Part 3. 结论**

CONTENT OF REPORT

- **Part 1. VIO 外参 / 时间差在线标定**
- **Part 2. 退化运动的可观性分析**
- **Part 3. 结论**

外参 / 时间差在线标定

Related Paper

VIORB

[1] Mur-Artal R, Tardós J D. Visual-inertial monocular SLAM with map reuse[J]. IEEE Robotics and Automation Letters, 2017, 2(2): 796-803.
[2] Huang W, Liu H. Online initialization and automatic camera-imu extrinsic calibration for monocular visual-inertial slam[C]//2018 IEEE International Conference on Robotics and Automation (ICRA). IEEE, 2018: 5182-5189.
[3] Campos C, MM M J, Tardós J D. Fast and Robust Initialization for Visual-Inertial SLAM[C]//2019 International Conference on Robotics and Automation (ICRA). IEEE, 2019: 1288-1294.

VINS

[4] Qin T, Shen S. Robust initialization of monocular visual-inertial estimation on aerial robots[C]//2017 IEEE/RSJ International Conference on Intelligent Robots and Systems (IROS). IEEE, 2017: 4225-4232.
[5] Ling Y, Bao L, Jie Z, et al. Modeling Varying Camera-IMU Time Offset in Optimization-Based Visual-Inertial Odometry[C]//Proceedings of the European Conference on Computer Vision (ECCV). 2018: 484-500.
[6] Liu J, Hu Z, Gao W. Online Temporal Calibration of Camera and IMU using Nonlinear Optimization[C]//2018 24th International Conference on Pattern Recognition (ICPR). IEEE, 2018: 1761-1766.
[7] Qin T, Shen S. Online temporal calibration for monocular visual-inertial systems[C]//2018 IEEE/RSJ International Conference on Intelligent Robots and Systems (IROS). IEEE, 2018: 3662-3669.

MSCKF

[8] Sun K, Mohta K, Pfrommer B, et al. Robust stereo visual inertial odometry for fast autonomous flight[J]. IEEE Robotics and Automation Letters, 2018, 3(2): 965-972.
[9] Li M, Mourikis A I. High-precision, consistent EKF-based visual-inertial odometry[J]. The International

外参 / 时间差在线标定

	文献	方法	精度 （来自论文）	适用场景
相对位姿在线标定	[4]	VINS基础上的相对位姿在线标定	旋转角误差：1° 平移误差：0.02m	1. 仅适用于基于非线性优化的VIO 2. 适用于相对位姿随时间缓慢变化的情况
	[2]	VI-ORB-SLAM基础上的相对位姿在线标定	旋转角误差：0.6° 平移误差：0.05m	1. 仅适用于基于非线性优化的VIO，且默认相对位姿在运行过程中基本不变 2. 计算量更小，适用于对计算量有限制的情况
时间差在线标定	[7]	基于像素点匀速运动的时间差标定方法	均方根误差： 0.68ms（真实值为30ms）	1. 仅适用于基于非线性优化的VIO 2. 表达式相对简单，适用于精度要求不是很高的情况
	[6]	将时间差变量加入IMU预积分表达式中	在数据集测试下误差小于基于像素点匀速运动的方法	1. 仅适用于基于非线性优化的VIO 2. 适用于对精度和收敛时间有更高要求的场合

[3] : MK-Solution -> First BA ->Second BA

外参 / 时间差在线标定

状态估计： P V Q ba bg λ

标定参数估计：
相机模型：内参标定 / 畸变系数标定 /tr
IMU 模型：三轴非正交矩阵 / 三轴尺度因子
VIO 模型：外参 / 时间差 td
双目模型：外参（基线）

个人心得：

1、**在线标定的原因：**一方面是因为标定本身存在误差，另一方面是因为传感器长时间使用外参也会发生改变；每次运行时间差 td 都不太相同，只能依靠在线标定的方法；合理的在线标定有利于精度的提升。

2、**状态估计的维度：**状态估计的参数不是越多越好，状态越多计算量越大，算法也越复杂；状态向量维度越高，系统自由度越大，系统的可观性会变差，状态估计精度也会变差。

3、**参数的敏感程度：** VIO 系统对不同参数的敏感程度是不一样的，对一些不太敏感的参数，系统很难精确的估计出其参数值来。

CONTENT OF REPORT

- **Part 1. VIO 外参 / 时间差在线标定**
- **Part 2. 退化运动的可观性分析**
- **Part 3. 结论**

可观性分析

论文分享

2019RAL:

Yang Y, Geneva P, Eckenhoff K, et al. Degenerate motion analysis for aided ins with online spatial and temporal sensor calibration[J]. IEEE Robotics and Automation Letters, 2019, 4(2): 2070-2077.

2018Tech.Rep.:

Y.Yang.P.Geneva,K.Eekenhoff,and G.Huang."Degenerate motion analysis for aided ins with online spatial and temporal sensor calibration."Tech.Rep..University of Delaware.Newark.DE,USA,2018. [Online].http://udel.edu/~yuyang/downloads/tr_calib.pdf

可观性分析

observability matrix：

$$\mathbf{M} = \begin{bmatrix} \mathbf{M}_1 \\ \mathbf{M}_2 \\ \vdots \\ \mathbf{M}_k \end{bmatrix} = \begin{bmatrix} \mathbf{H}_1\mathbf{\Phi}(1,1) \\ \mathbf{H}_2\mathbf{\Phi}(2,1) \\ \vdots \\ \mathbf{H}_k\mathbf{\Phi}(k,1) \end{bmatrix}$$

$$\mathbf{x} = \begin{bmatrix} \mathbf{x}_I^\top & \mathbf{x}_{calib}^\top & t_d & \mathbf{x}_\mathbf{f}^\top \end{bmatrix}^\top$$

System Dynamical Model：

$$\begin{aligned} {}^I_G\dot{\bar{q}}(t) &= \frac{1}{2}\mathbf{\Omega}\left({}^I\boldsymbol{\omega}(t)\right){}^I_G\bar{q}(t) \\ {}^G\dot{\mathbf{p}}_I(t) &= {}^G\mathbf{v}_I(t), \quad {}^G\dot{\mathbf{v}}_I(t) = {}^G\mathbf{a}(t) \\ \dot{\mathbf{b}}_g(t) &= \mathbf{n}_{wg}(t), \quad \dot{\mathbf{b}}_a(t) = \mathbf{n}_{wa}(t) \\ \dot{\mathbf{x}}_{calib}(t) &= \mathbf{0}_{6\times1}, \quad \dot{t}_d(t) = 0, \quad \dot{\mathbf{x}}_\mathbf{f}(t) = \mathbf{0}_{3\times1} \end{aligned}$$

state transition matrix：

$\Phi(k,1)$

Measurement Model：

$$\begin{aligned} \mathbf{z}_C &= \underbrace{\begin{bmatrix} \lambda_r & \mathbf{0}_{1\times2} \\ \mathbf{0}_{2\times1} & \lambda_b\mathbf{I}_2 \end{bmatrix}}_{\mathbf{\Lambda}} \begin{bmatrix} z^{(r)} \\ \mathbf{z}^{(b)} \end{bmatrix} = \mathbf{\Lambda}\begin{bmatrix} \sqrt{{}^C\mathbf{p}_\mathbf{f}{}^\top{}^C\mathbf{p}_\mathbf{f}} + n^{(r)} \\ \mathbf{h_b}\left({}^C\mathbf{p}_\mathbf{f}, \mathbf{n}^{(b)}\right) \end{bmatrix} \\ &\simeq \mathbf{\Lambda}\begin{bmatrix} \mathbf{H}_r{}^C\tilde{\mathbf{p}}_\mathbf{f} + n^{(r)} \\ \mathbf{H}_b{}^C\tilde{\mathbf{p}}_\mathbf{f} + \mathbf{H}_n\mathbf{n}^{(b)} \end{bmatrix} \end{aligned}$$

Measurement Jacobian：

$\mathrm{H_k}$

$${}^C\mathbf{p}_\mathbf{f} = {}^C_I\mathbf{R}\,{}^I_G\mathbf{R}(t-t_d)\left({}^G\mathbf{p}_\mathbf{f} - {}^G\mathbf{p}_I(t-t_d)\right) + {}^C\mathbf{p}_I$$

状态转移矩阵

$$\Phi_k = \Phi(t_{k+1}, t_k) = \exp\left(\int_{t_k}^{t_{k+1}} \mathbf{F}_c(\tau)\mathrm{d}\tau\right)$$

$$\Phi_n = \exp(F\delta t) \approx I + F\delta t + \frac{1}{2}(F\delta t)^2 + \frac{1}{6}(F\delta t)^3$$

state transition matrix：

$$\mathbf{\Phi}(k,1) = \begin{bmatrix} \mathbf{\Phi}_{I(k,1)} & \mathbf{0}_{15\times 6} & \mathbf{0}_{15\times 1} & \mathbf{0}_{15\times 3} \\ \mathbf{0}_{6\times 15} & \mathbf{\Phi}_{Calib(k,1)} & \mathbf{0}_{5\times 1} & \mathbf{0}_{6\times 3} \\ \mathbf{0}_{1\times 15} & \mathbf{0}_{1\times 6} & \mathbf{\Phi}_{t_d(k,1)} & \mathbf{0}_{1\times 3} \\ \mathbf{0}_{3\times 15} & \mathbf{0}_{3\times 6} & \mathbf{0}_{3\times 1} & \mathbf{\Phi}_{\mathrm{f}(k,1)} \end{bmatrix}$$

其中：

$$\mathbf{\Phi}_{I(k,1)} = \begin{bmatrix} \mathbf{\Phi}_{I11} & \mathbf{\Phi}_{I12} & \mathbf{0}_3 & \mathbf{0}_3 & \mathbf{0}_3 \\ \mathbf{0}_3 & \mathbf{I}_3 & \mathbf{0}_3 & \mathbf{0}_3 & \mathbf{0}_3 \\ \mathbf{\Phi}_{I31} & \mathbf{\Phi}_{I32} & \mathbf{I}_3 & \mathbf{\Phi}_{I34} & \mathbf{0}_3 \\ \mathbf{0}_3 & \mathbf{0}_3 & \mathbf{0}_3 & \mathbf{I}_3 & \mathbf{0}_3 \\ \mathbf{\Phi}_{I51} & \mathbf{\Phi}_{I52} & \mathbf{\Phi}_{I53} & \mathbf{\Phi}_{I54} & \mathbf{I}_3 \end{bmatrix}, \ \mathbf{\Phi}_{Calib(k,1)} = \mathbf{I}_6, \ \mathbf{\Phi}_{t_d(k,1)} = 1 \text{ and } \mathbf{\Phi}_{\mathrm{f}(k,1)} = \mathbf{I}_3$$

根据矩阵微分方程来计算**状态转移矩阵**：

$$\dot{\mathbf{\Phi}}(t, t_0) = \mathbf{F}_c(t)\mathbf{\Phi}(t, t_0)$$

其中 Fc(t) 是连续时间**误差状态转移矩阵**：

$$\mathbf{F}_c(t) = \begin{bmatrix} -\lfloor \hat{\omega} \times \rfloor & -\mathbf{I}_3 & \mathbf{0}_3 & \mathbf{0}_3 & \mathbf{0}_3 \\ \mathbf{0}_3 & \mathbf{0}_3 & \mathbf{0}_3 & \mathbf{0}_3 & \mathbf{0}_3 \\ -\mathbf{C}^T({}^I\hat{\bar{q}}_G)\lfloor \hat{\mathbf{a}} \times \rfloor & \mathbf{0}_3 & \mathbf{0}_3 & -\mathbf{C}^T({}^I\hat{\bar{q}}_G) & \mathbf{0}_3 \\ \mathbf{0}_3 & \mathbf{0}_3 & \mathbf{0}_3 & \mathbf{0}_3 & \mathbf{0}_3 \\ \mathbf{0}_3 & \mathbf{0}_3 & \mathbf{I}_3 & \mathbf{0}_3 & \mathbf{0}_3 \end{bmatrix}$$

[1] Hesch J A, Kottas D G, Bowman S L, et al. Consistency analysis and improvement of vision-aided inertial navigation[J]. IEEE Transactions on Robotics, 2013, 30(1): 158-176.

[2] J. A. Hesch, D. G. Kottas, S. L. Bowman, and S. I. Roumeliotis. Observability-constrained vision-aided inertial navigation. Technical Report 2012-001, University of Minnesota, Dept.of Comp. Sci. & Eng., MARS Lab, Feb. 2012.

状态转移矩阵

推导过程（部分）：

9.1.1 The structure of $\Phi(t,t_0)$

To simplify our derivation, we will first show that $\Phi(t,t_0)$ has the structure (omitting the time parameters here for clarity)

$$\Phi(t,t_0)=\begin{bmatrix}\Phi_{11}&\Phi_{12}&\Phi_{13}&\Phi_{14}&\Phi_{15}&\Phi_{16}\\ \Phi_{21}&\Phi_{22}&\Phi_{23}&\Phi_{24}&\Phi_{25}&\Phi_{26}\\ \Phi_{31}&\Phi_{32}&\Phi_{33}&\Phi_{34}&\Phi_{35}&\Phi_{36}\\ \Phi_{41}&\Phi_{42}&\Phi_{43}&\Phi_{44}&\Phi_{45}&\Phi_{46}\\ \Phi_{51}&\Phi_{52}&\Phi_{53}&\Phi_{54}&\Phi_{55}&\Phi_{56}\\ \Phi_{61}&\Phi_{62}&\Phi_{63}&\Phi_{64}&\Phi_{65}&\Phi_{66}\end{bmatrix}=\begin{bmatrix}\Phi_{11}&\Phi_{12}&\mathbf{0}_3&\mathbf{0}_3&\mathbf{0}_3&\mathbf{0}_3\\ \mathbf{0}_3&\mathbf{I}_3&\mathbf{0}_3&\mathbf{0}_3&\mathbf{0}_3&\mathbf{0}_3\\ \Phi_{31}&\Phi_{32}&\mathbf{I}_3&\Phi_{34}&\mathbf{0}_3&\mathbf{0}_3\\ \mathbf{0}_3&\mathbf{0}_3&\mathbf{0}_3&\mathbf{I}_3&\mathbf{0}_3&\mathbf{0}_3\\ \Phi_{51}&\Phi_{52}&\Phi_{53}&\Phi_{54}&\mathbf{I}_3&\mathbf{0}_3\\ \mathbf{0}_3&\mathbf{0}_3&\mathbf{0}_3&\mathbf{0}_3&\mathbf{0}_3&\mathbf{I}_3\end{bmatrix} \tag{43}$$

To show this structure, we take advantage of the $\mathbf{F}_c$ matrix structure. Specifically, notice that its second and fourth rows are zero; from (41), we then have

$$\dot{\Phi}_{2,:}(t,t_0)=\mathbf{0} \tag{44}$$

So we see that the block row $\Phi_{2,:}$ is constant for all t. Then, because the block matrix $\Phi_{2,j}(t_0,t_0)$ is $\mathbf{I}_3$ if $j=2$ or $\mathbf{0}_3$ if $j\neq 2$, we then have

$$\Phi_{2,j}=\mathbf{0}_3\ \ \forall j\neq 2 \tag{45}$$

$$\Phi_{2,2}=\mathbf{I}_3 \tag{46}$$

Using the same observation, we can reveal the elements of $\Phi_{4,:}$

$$\dot{\Phi}_{4,:}(t,t_0)=\mathbf{0}\implies\Phi_{4j}(t,t_0)=\mathbf{0} \tag{47}$$

for $j\neq 4$, while

$$\Phi_{44}(t,t_0)=\mathbf{I}_3 \tag{48}$$

雅克比矩阵

Measurement Jacobian：

$$\mathbf{H}_C = \frac{\partial \tilde{\mathbf{z}}_C}{\partial \tilde{\mathbf{x}}} = \frac{\partial \tilde{\mathbf{z}}_C}{\partial {}^C\tilde{\mathbf{p}}_\mathbf{f}} \frac{\partial {}^C\tilde{\mathbf{p}}_\mathbf{f}}{\partial \tilde{\mathbf{x}}} = \mathbf{H}_{proj} \frac{\partial {}^C\tilde{\mathbf{p}}_\mathbf{f}}{\partial \tilde{\mathbf{x}}}$$
$$= \mathbf{H}_{proj} \begin{bmatrix} \frac{\partial {}^C\tilde{\mathbf{p}}_\mathbf{f}}{\partial \tilde{\mathbf{x}}_I} & \frac{\partial {}^C\tilde{\mathbf{p}}_\mathbf{f}}{\partial \tilde{\mathbf{x}}_{calib}} & \frac{\partial {}^C\tilde{\mathbf{p}}_\mathbf{f}}{\partial \tilde{t}_d} & \frac{\partial {}^C\tilde{\mathbf{p}}_\mathbf{f}}{\partial \tilde{\mathbf{x}}_\mathbf{f}} \end{bmatrix}$$

$$\frac{\partial {}^C\tilde{\mathbf{p}}_\mathbf{f}}{\partial \delta\boldsymbol{\theta}} = {}^C_I\hat{\mathbf{R}}\,{}^{I_k}_G\hat{\mathbf{R}}\,\hat{\mathbf{R}}\lfloor({}^G\hat{\mathbf{p}}_\mathbf{f} - {}^G\hat{\mathbf{p}}_{I_k})\rfloor\,{}^G_{I_k}\hat{\mathbf{R}}$$

$$\frac{\partial {}^C\tilde{\mathbf{p}}_\mathbf{f}}{\partial {}^G\tilde{\mathbf{p}}_{I_k}} = -{}^C_I\hat{\mathbf{R}}\,{}^{I_k}_G\hat{\mathbf{R}}, \quad \frac{\partial {}^C\tilde{\mathbf{p}}_\mathbf{f}}{\partial {}^G\tilde{\mathbf{p}}_\mathbf{f}} = {}^C_I\hat{\mathbf{R}}\,{}^{I_k}_G\hat{\mathbf{R}}$$

$$\frac{\partial {}^C\tilde{\mathbf{p}}_\mathbf{f}}{\partial \delta\boldsymbol{\theta}_c} = {}^C_I\hat{\mathbf{R}}\,{}^{I_k}_G\hat{\mathbf{R}}\,\hat{\mathbf{R}}\lfloor({}^G\hat{\mathbf{p}}_\mathbf{f} - {}^G\hat{\mathbf{p}}_{I_k})\rfloor\,{}^G_{I_k}\hat{\mathbf{R}}\,{}^I_C\hat{\mathbf{R}}$$

$$\frac{\partial {}^C\tilde{\mathbf{p}}_\mathbf{f}}{\partial {}^C\tilde{\mathbf{p}}_I} = {}^C_I\hat{\mathbf{R}}\,{}^{I_k}_G\hat{\mathbf{R}}\,{}^G_{I_k}\hat{\mathbf{R}}\,{}^I_C\hat{\mathbf{R}} = \mathbf{I}_3$$

$$\frac{\partial {}^C\tilde{\mathbf{p}}_\mathbf{f}}{\partial \tilde{t}_d} = {}^C_I\hat{\mathbf{R}}\,{}^{I_k}_G\hat{\mathbf{R}}\left(-\lfloor({}^G\hat{\mathbf{p}}_\mathbf{f} - {}^G\hat{\mathbf{p}}_{I_k})\rfloor\,{}^G_{I_k}\hat{\mathbf{R}}\,{}^{I_k}\hat{\boldsymbol{\omega}} + {}^G\hat{\mathbf{v}}_{I_k}\right)$$

雅克比矩阵

推导过程：

$$ {}^{C}p_f = {}^{C}_{I}R\,{}^{I}_{G}R\left(t-t_d\right)\left({}^{G}p_f - {}^{G}p_I\left(t-t_d\right)\right) + {}^{C}p_I $$

$\frac{\partial {}^{C}\tilde{\mathbf{p}}_{\mathbf{f}}}{\partial \delta\boldsymbol{\theta}}$：

$$
\begin{aligned}
{}^{C}\mathbf{p}_{\mathbf{f}} &= {}^{C}\hat{\mathbf{p}}_{\mathbf{f}} + {}^{C}\tilde{\mathbf{p}}_{\mathbf{f}} = {}^{C}_{I}\hat{\mathbf{R}}\left(\mathbf{I} - \lfloor\delta\boldsymbol{\theta}\rfloor\right){}^{I_k}_{G}\hat{\mathbf{R}}\left({}^{G}\hat{\mathbf{p}}_{\mathbf{f}} - {}^{G}\hat{\mathbf{p}}_{I_k}\right) + {}^{C}\hat{\mathbf{p}}_{I} \\
\Rightarrow {}^{C}\tilde{\mathbf{p}}_{\mathbf{f}} &= {}^{C}_{I}\hat{\mathbf{R}}\lfloor{}^{I_k}_{G}\hat{\mathbf{R}}\left({}^{G}\hat{\mathbf{p}}_{\mathbf{f}} - {}^{G}\hat{\mathbf{p}}_{I_k}\right)\rfloor\delta\boldsymbol{\theta} = {}^{C}_{I}\hat{\mathbf{R}}\,{}^{I_k}_{G}\hat{\mathbf{R}}\lfloor\left({}^{G}\hat{\mathbf{p}}_{\mathbf{f}} - {}^{G}\hat{\mathbf{p}}_{I_k}\right)\rfloor{}^{G}_{I_k}\hat{\mathbf{R}}\delta\boldsymbol{\theta} \\
\Rightarrow \frac{\partial {}^{C}\tilde{\mathbf{p}}_{\mathbf{f}}}{\partial \delta\boldsymbol{\theta}} &= {}^{C}_{I}\hat{\mathbf{R}}\,{}^{I_k}_{G}\hat{\mathbf{R}}\lfloor\left({}^{G}\hat{\mathbf{p}}_{\mathbf{f}} - {}^{G}\hat{\mathbf{p}}_{I_k}\right)\rfloor{}^{G}_{I_k}\hat{\mathbf{R}}
\end{aligned}
$$

$\frac{\partial {}^{C}\tilde{\mathbf{p}}_{\mathbf{f}}}{\partial {}^{G}\tilde{\mathbf{p}}_{\mathbf{f}}}$：

$$
\begin{aligned}
{}^{C}\mathbf{p}_{\mathbf{f}} &= {}^{C}\hat{\mathbf{p}}_{\mathbf{f}} + {}^{C}\tilde{\mathbf{p}}_{\mathbf{f}} = {}^{C}_{I}\hat{\mathbf{R}}\,{}^{I_k}_{G}\hat{\mathbf{R}}\left({}^{G}\hat{\mathbf{p}}_{\mathbf{f}} + {}^{G}\tilde{\mathbf{p}}_{\mathbf{f}} - {}^{G}\hat{\mathbf{p}}_{I_k}\right) + {}^{C}\hat{\mathbf{p}}_{I} \\
\Rightarrow {}^{C}\tilde{\mathbf{p}}_{\mathbf{f}} &= {}^{C}_{I}\hat{\mathbf{R}}\,{}^{I_k}_{G}\hat{\mathbf{R}}\,{}^{G}\tilde{\mathbf{p}}_{\mathbf{f}} \\
\Rightarrow \frac{\partial {}^{C}\tilde{\mathbf{p}}_{\mathbf{f}}}{\partial {}^{G}\tilde{\mathbf{p}}_{\mathbf{f}}} &= {}^{C}_{I}\hat{\mathbf{R}}\,{}^{I_k}_{G}\hat{\mathbf{R}}
\end{aligned}
$$

$\frac{\partial {}^{C}\tilde{\mathbf{p}}_{f}}{\partial {}^{G}\tilde{\mathbf{p}}_{I_k}}$：

$$
\begin{aligned}
{}^{C}\mathbf{p}_{\mathbf{f}} &= {}^{C}\hat{\mathbf{p}}_{\mathbf{f}} + {}^{C}\tilde{\mathbf{p}}_{\mathbf{f}} = {}^{C}_{I}\hat{\mathbf{R}}\,{}^{I_k}_{G}\hat{\mathbf{R}}\left({}^{G}\hat{\mathbf{p}}_{\mathbf{f}} - {}^{G}\hat{\mathbf{p}}_{I_k} - {}^{G}\tilde{\mathbf{p}}_{I_k}\right) + {}^{C}\hat{\mathbf{p}}_{I} \\
\Rightarrow {}^{C}\tilde{\mathbf{p}}_{\mathbf{f}} &= -{}^{C}_{I}\hat{\mathbf{R}}\,{}^{I_k}_{G}\hat{\mathbf{R}}\,{}^{G}\tilde{\mathbf{p}}_{I_k} \\
\Rightarrow \frac{\partial {}^{C}\tilde{\mathbf{p}}_{f}}{\partial {}^{G}\tilde{\mathbf{p}}_{I_k}} &= -{}^{C}_{I}\hat{\mathbf{R}}\,{}^{I_k}_{G}\hat{\mathbf{R}}
\end{aligned}
$$

雅克比矩阵

推导过程：

$$ {}^{C}p_f = {}^{C}_{I}R\left({}^{I}_{G}R\left(t-t_d\right)\left({}^{G}p_f - {}^{G}p_I\left(t-t_d\right)\right)\right) + {}^{C}p_I $$

$\frac{\partial^C \tilde{\mathbf{p}}_\mathbf{f}}{\partial \delta \boldsymbol{\theta}_c}$ ：

$$ {}^{C}\mathbf{p}_\mathbf{f} = {}^{C}\hat{\mathbf{p}}_\mathbf{f} + {}^{C}\tilde{\mathbf{p}}_\mathbf{f} = \left(\mathbf{I}_3 - \lfloor \delta\boldsymbol{\theta}_c \rfloor\right) {}^{C}_{I}\hat{\mathbf{R}}\,{}^{I_k}_{G}\hat{\mathbf{R}}\left({}^{G}\hat{\mathbf{p}}_\mathbf{f} - {}^{G}\hat{\mathbf{p}}_{I_k}\right) + {}^{C}\hat{\mathbf{p}}_I $$

$$ \Rightarrow {}^{C}\tilde{\mathbf{p}}_\mathbf{f} = \lfloor {}^{C}_{I}\hat{\mathbf{R}}\,{}^{I_k}_{G}\hat{\mathbf{R}}\left({}^{G}\hat{\mathbf{p}}_\mathbf{f} - {}^{G}\hat{\mathbf{p}}_{I_k}\right) \rfloor \delta\boldsymbol{\theta}_c $$

$$ \Rightarrow \frac{\partial^C \tilde{\mathbf{p}}_\mathbf{f}}{\partial \delta \boldsymbol{\theta}_c} = \lfloor {}^{C}_{I}\hat{\mathbf{R}}\,{}^{I_k}_{G}\hat{\mathbf{R}}\left({}^{G}\hat{\mathbf{p}}_\mathbf{f} - {}^{G}\hat{\mathbf{p}}_{I_k}\right) \rfloor $$

$\frac{\partial^C \tilde{\mathbf{p}}_\mathbf{f}}{\partial^C \tilde{\mathbf{p}}_I}$ ：

$$ {}^{C}p_f = {}^{C}\hat{p}_f + {}^{C}\tilde{p}_f = {}^{C}_{I}\hat{R}\left({}^{I}_{G}R\left({}^{G}p_f - {}^{G}p_I\right) + {}^{C}p_I\right) + {}^{C}\tilde{p}_f $$

$$ \Rightarrow \frac{\partial^C \tilde{\mathbf{p}}_\mathbf{f}}{\partial^C \tilde{\mathbf{p}}_I} = \mathbf{I}_3 $$

雅克比矩阵

推导过程：

$$ {}^{C}p_f = {}^{C}_{I}R\,{}^{I}_{G}R\left(t-t_d\right)\left({}^{G}p_f - {}^{G}p_I\left(t-t_d\right)\right) + {}^{C}p_I $$

$\dfrac{\partial {}^{C}\tilde{p}_f}{\partial \tilde{t}_d}$ ：

$$ {}^{C}p_f = {}^{C}\hat{p}_f + {}^{C}\delta p_f = {}^{C}_{I}\hat{R}\,{}^{I}_{G}R\left(t-\left(\hat{t}_d+\delta t_d\right)\right)\left({}^{G}\hat{p}_f - {}^{G}p_I\left(t-\left(t_d+\delta t_d\right)\right)\right) + {}^{C}p_I $$

$$ = {}^{C}_{I}\hat{R}\left(I-\left[\hat{\omega}\left(t-\hat{t}_d\right)\times\right]\delta t_d\right){}^{I}_{G}R\left({}^{G}p_f - \left({}^{G}p_I\left(t-t_d\right)+{}^{G}\hat{v}_f\,\delta t_d\right)\right) + {}^{C}p_I $$

$$ = {}^{C}_{I}\hat{R}\,{}^{I}_{G}R\left({}^{G}\hat{p}_f - {}^{G}p_I\left(t-\hat{t}_d\right)+{}^{G}\hat{v}_f\,\delta t_d\right) + {}^{C}_{I}R\left[\omega\left(t-t_d\right)\times\right]\delta t_d\,{}^{I}_{G}R\left({}^{G}\hat{p}_f - {}^{G}p_I\left(t-\hat{t}_d\right)+{}^{G}\hat{v}_f\,\delta t_d\right) + {}^{C}p_I $$

$$ = {}^{C}_{I}\hat{R}\,{}^{I}_{G}\hat{R}\left({}^{G}\hat{p}_f - {}^{G}p_I\right) + {}^{C}_{I}\hat{R}\,{}^{I}_{G}R\,{}^{G}\hat{v}_f\,\delta t_d + {}^{C}_{I}R\left[\hat{\omega}\delta t_d\times\right]{}^{I}_{G}R\left({}^{G}p_f - {}^{G}p_I\right) + {}^{C}p_I $$

$$ + {}^{C}_{I}\hat{R}\left[{}^{G}\hat{v}_f\,\delta t_d\times\right]\omega\delta t_d \qquad \left(\delta t_d^2\right) $$

$$ \delta {}^{C}p_f = {}^{C}_{I}\hat{R}\,{}^{I}_{G}\hat{R}\,{}^{G}\hat{v}_f\,\delta t_d + {}^{C}_{I}R\left[\hat{\omega}\delta t_d\times\right]{}^{I}_{G}R\left({}^{G}p_f - {}^{G}p_I\right) $$

$$ \delta p = -\delta\rho $$

$$ = -{}^{C}_{I}\hat{R}\,{}^{I}_{G}R\,{}^{G}\hat{v}_f\,\delta t_d + {}^{C}_{I}R\left[{}^{G}\hat{p}_f - {}^{G}p_I\right]\times\omega\delta t_d $$

$$ \delta R = R\left[\delta\theta\times\right] \quad R^{T} $$

$$ = -{}^{C}_{I}\hat{R}\,{}^{I}_{G}R\,{}^{G}\hat{v}_f\,\delta t_d + {}^{C}_{I}R\,{}^{I}_{G}R\left[{}^{G}\hat{p}_f - {}^{G}p_I\right]\times{}^{G}_{I_k}R\,\omega\delta t_d $$

$$ = {}^{C}_{I}\hat{R}\,{}^{I}_{G}R\left(-\left[{}^{G}\hat{p}_f - {}^{G}p_I\right]\times{}^{G}_{I_k}\hat{R}\,\omega + {}^{G}\hat{v}_f\right)\delta t_d $$

$$ \frac{\delta {}^{C}p_f}{\delta t_d} = {}^{C}_{I}\hat{R}\,{}^{I}_{G}R\left(-\left[{}^{G}\hat{p}_f - {}^{G}p_I\right]\times{}^{G}_{I_k}R\,\omega + {}^{G}\hat{v}_f\right) $$

可观性分析

Table 1: Observability of spatial and temporal calibration of aided INS with different motions

Motion	**Unobservable**	**Observable**
No motion	${}^{C}\mathbf{p}_I$, ${}^{C}_{I}\mathbf{R}$ and t_d	–
Pure Translation	${}^{C}\mathbf{p}_I$	${}^{C}_{I}\mathbf{R}$ and t_d
One-axis Rotation	${}^{C}\mathbf{p}_I$ along rotation axis	${}^{C}_{I}\mathbf{R}$ and t_d
Constant ${}^{I}\boldsymbol{\omega}$ Constant ${}^{I}\mathbf{v}$	t_d and ${}^{C}\mathbf{p}_I$ along rotation axis	${}^{C}_{I}\mathbf{R}$
Constant ${}^{I}\boldsymbol{\omega}$ Constant ${}^{G}\mathbf{a}$	t_d and ${}^{C}\mathbf{p}_I$ along rotation axis	${}^{C}_{I}\mathbf{R}$
One global axis translation Two-axis rotation	–	${}^{C}_{I}\mathbf{R}$, ${}^{C}\mathbf{p}_I$, t_d
Random motion	–	${}^{C}_{I}\mathbf{R}$, ${}^{C}\mathbf{p}_I$, t_d

四种退化运动

可观性分析

Summary：

1. 显然，与平移校准相比，**方向校准的可观性对不同的运动不太敏感**，并且在大多数情况下都是可观的。

2. 通常，**辅助传感器的纯三轴旋转**不是校准参数的退化运动，而是对于**其他状态变量可能是退化的**；例如，单目相机的纯旋转会导致特征尺度的损失。

3. 为了获得**可靠的平移校准，需要至少两轴旋转（随机平移）**。然而，在这里我们通过分析显示单轴旋转将导致平移校准沿旋转轴变得不可观，进一步提高了我们的理解。

4. 可靠的空间和时间校准的最小运动**要求是至少一个全局轴平移和双轴旋转**，并且**不建议在平面运动下执行在线 IMU 相机校准**（例如，用于自动驾驶的平面 VINS ）。

5. 有趣的是，除了非常严格的运动外，**时间偏移校准通常是可观的**。我们想再次指出，这些发现不仅对于成功进行空间和时间传感器校准很重要，而且对于监测估计器的正常运行状况也很有用（如果经历退化运动，系统应该被警告）。

6. 如果校准参数是可观的（例如**在随机运动下**），则**额外的全局测量将有助于提高校准精度**，因为它们可以使导航系统可观。

7. 但是，如果系统在退化运动状态下进行校准，则额外的全局测量将无法使标定参数可观，**不能简单的认**

可观性分析

4.1 Pure Translation （No Rotation）

引理 1. 如果辅助 INS 经历纯平移 (无旋转) ，则空间校准的平移部分 p 将是不可的，具有不可观的方向，如：

$$\mathbf{N}_{pt} = \begin{bmatrix} \mathbf{0}_{3\times 15} & \mathbf{0}_3 & \mathbf{I}_3 & \mathbf{0}_{3\times 1} & -({}^{G}_{I_1}\hat{\mathbf{R}}\,{}^{I}_{C}\hat{\mathbf{R}})^{\top} \end{bmatrix}^{\top}$$

证明：对应纯平移，对任意的 k 我们都有：

$${}^{G}_{I_k}\mathbf{R} = {}^{G}_{I_1}\mathbf{R}\,{}^{I_1}_{I_k}\mathbf{R} = {}^{G}_{I_1}\mathbf{R}\mathbf{I}_3 = {}^{G}_{I_1}\mathbf{R}$$

因此有：

$$\mathbf{M}_k\mathbf{N}_{pt} = \mathbf{\Xi}_k\left({}^{G}_{I_k}\mathbf{R}\,{}^{I}_{C}\hat{\mathbf{R}} - {}^{G}_{I_1}\mathbf{R}\,{}^{I}_{C}\hat{\mathbf{R}}\right) = \mathbf{0}$$

$$\Rightarrow \mathbf{M}\mathbf{N}_{pt} = \mathbf{0}$$

为了几何解释这个不可观的方向，我们用↷ p 扰乱校准平移：

$${}^{C}\mathbf{p}'_I = {}^{C}\mathbf{p}_I + \delta\mathbf{p}$$

沿着该零空间的相应特征位置变化可以被建模为：

$${}^{G}\mathbf{p}'_{\mathbf{f}} = {}^{G}\mathbf{p}_{\mathbf{f}} - {}^{G}_{I_1}\hat{\mathbf{R}}\,{}^{I}_{C}\hat{\mathbf{R}}\delta\mathbf{p}$$

因此有：

$$\begin{aligned} {}^{C}\mathbf{p}'_{\mathbf{f}} &= {}^{C}_{I}\mathbf{R}\,{}^{I_k}_{G}\mathbf{R}\left({}^{G}\mathbf{p}'_{\mathbf{f}} - {}^{G}\mathbf{p}_{I_k}\right) + {}^{C}\mathbf{p}'_I \\ &= {}^{C}_{I}\mathbf{R}\,{}^{I_k}_{G}\mathbf{R}\left({}^{G}\mathbf{p}_{\mathbf{f}} - {}^{G}\mathbf{p}_{I_k}\right) + {}^{C}\mathbf{p}_I \\ &= {}^{C}\mathbf{p}_{\mathbf{f}} \end{aligned}$$

$$\mathbf{\Xi}_{\mathbf{\Gamma}k} = \begin{bmatrix} \mathbf{\Gamma}_1 & \mathbf{\Gamma}_2 & -\mathbf{I}_3\delta t_k & \mathbf{\Gamma}_3 & -\mathbf{I}_3 & \mathbf{\Gamma}_4 & {}^{G}_{I_k}\hat{\mathbf{R}}\,{}^{I}_{C}\hat{\mathbf{R}} & \mathbf{\Gamma}_5 & \mathbf{I}_3 \end{bmatrix}$$

$$\mathbf{\Gamma}_1 = \lfloor {}^{G}\hat{\mathbf{p}}_{\mathbf{f}} - {}^{G}\hat{\mathbf{p}}_{I_1} - {}^{G}\hat{\mathbf{p}}_{I_1}\delta t_k - \frac{1}{2}{}^{G}\mathbf{g}\delta t_k^2 \rfloor {}^{G}_{I_1}\hat{\mathbf{R}}$$

$$\mathbf{\Gamma}_2 = \lfloor {}^{G}\hat{\mathbf{p}}_{\mathbf{f}} - {}^{G}\hat{\mathbf{p}}_{I_k} \rfloor {}^{G}_{I_k}\hat{\mathbf{R}}\mathbf{\Phi}_{I12} - \mathbf{\Phi}_{I52}$$

$$\mathbf{\Gamma}_3 = -\mathbf{\Phi}_{I54},\ \mathbf{\Gamma}_4 = \lfloor {}^{G}\hat{\mathbf{p}}_{\mathbf{f}} - {}^{G}\hat{\mathbf{p}}_{I_k} \rfloor {}^{G}_{I_k}\hat{\mathbf{R}}\,{}^{I}_{C}\hat{\mathbf{R}}$$

$$\mathbf{\Gamma}_5 = -\lfloor ({}^{G}\hat{\mathbf{p}}_{\mathbf{f}} - {}^{G}\hat{\mathbf{p}}_{I_k}) \rfloor {}^{G}_{I_k}\hat{\mathbf{R}}\,{}^{I_k}\hat{\boldsymbol{\omega}} + {}^{G}\hat{\mathbf{v}}_{I_k}$$

$${}^{C}\mathbf{p}_{\mathbf{f}} = {}^{C}_{I}\mathbf{R}\,{}^{I}_{G}\mathbf{R}(t-t_d)\left({}^{G}\mathbf{p}_{\mathbf{f}} - {}^{G}\mathbf{p}_I(t-t_d)\right) + {}^{C}\mathbf{p}_I$$

很明显，在给定特征测量（11）的情况下，**系统无法识别这种扰动↷ p 到 p**，因此 Npt 与 IMU 传感器平移部分有关，这意味着如果没有旋转，空间校准的平移参数是不可观的。

可观性分析

Monte-Carlo simulations:

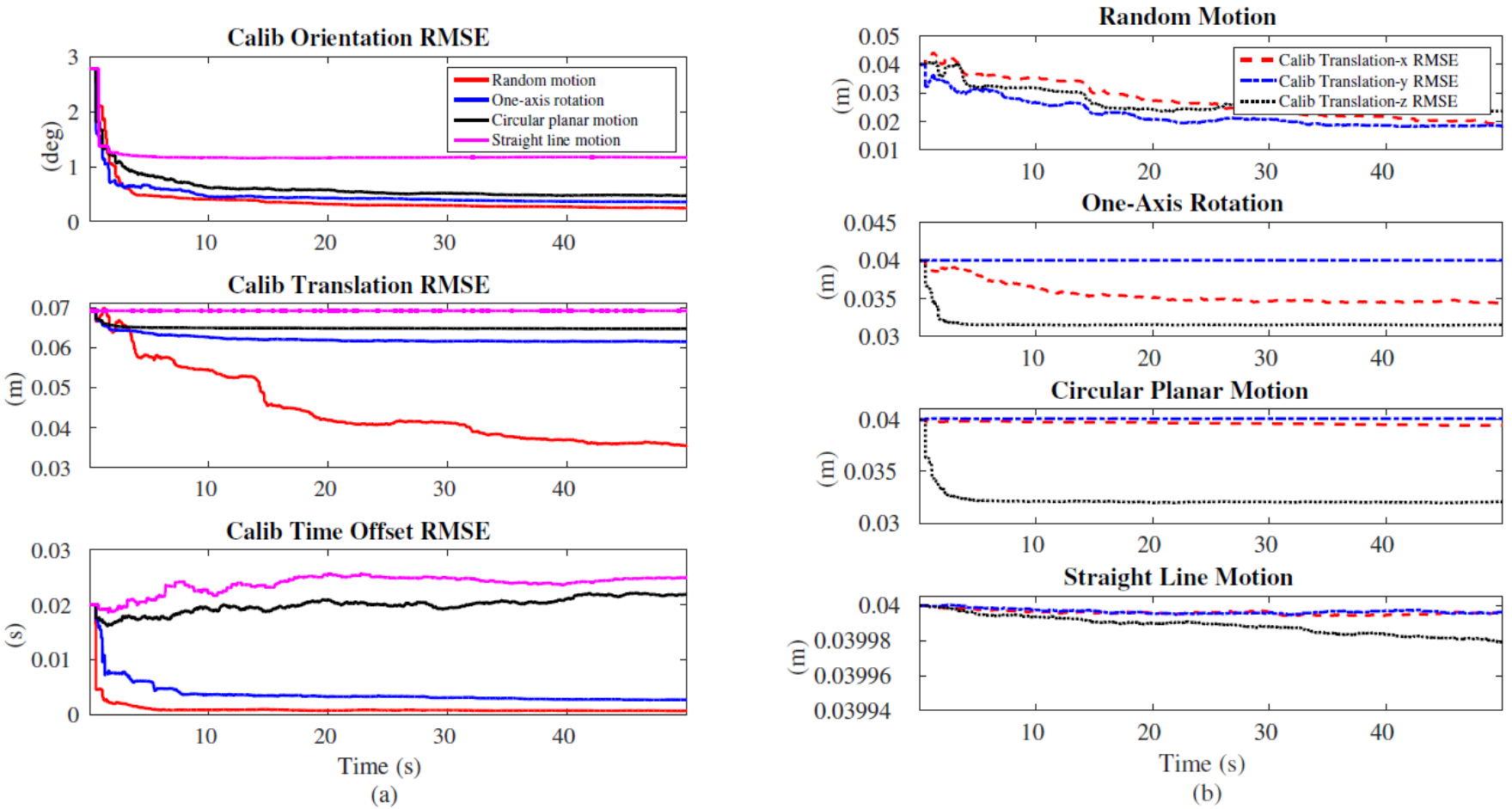

图 4： 在所有考虑的运动情况下 (td=0.04(sec)) 的空间和时间校准的模拟平均 RMSE

（a）时空参数的校准误差　　（b）空间校准的三轴平移误差

可观性分析

Experimental Results:

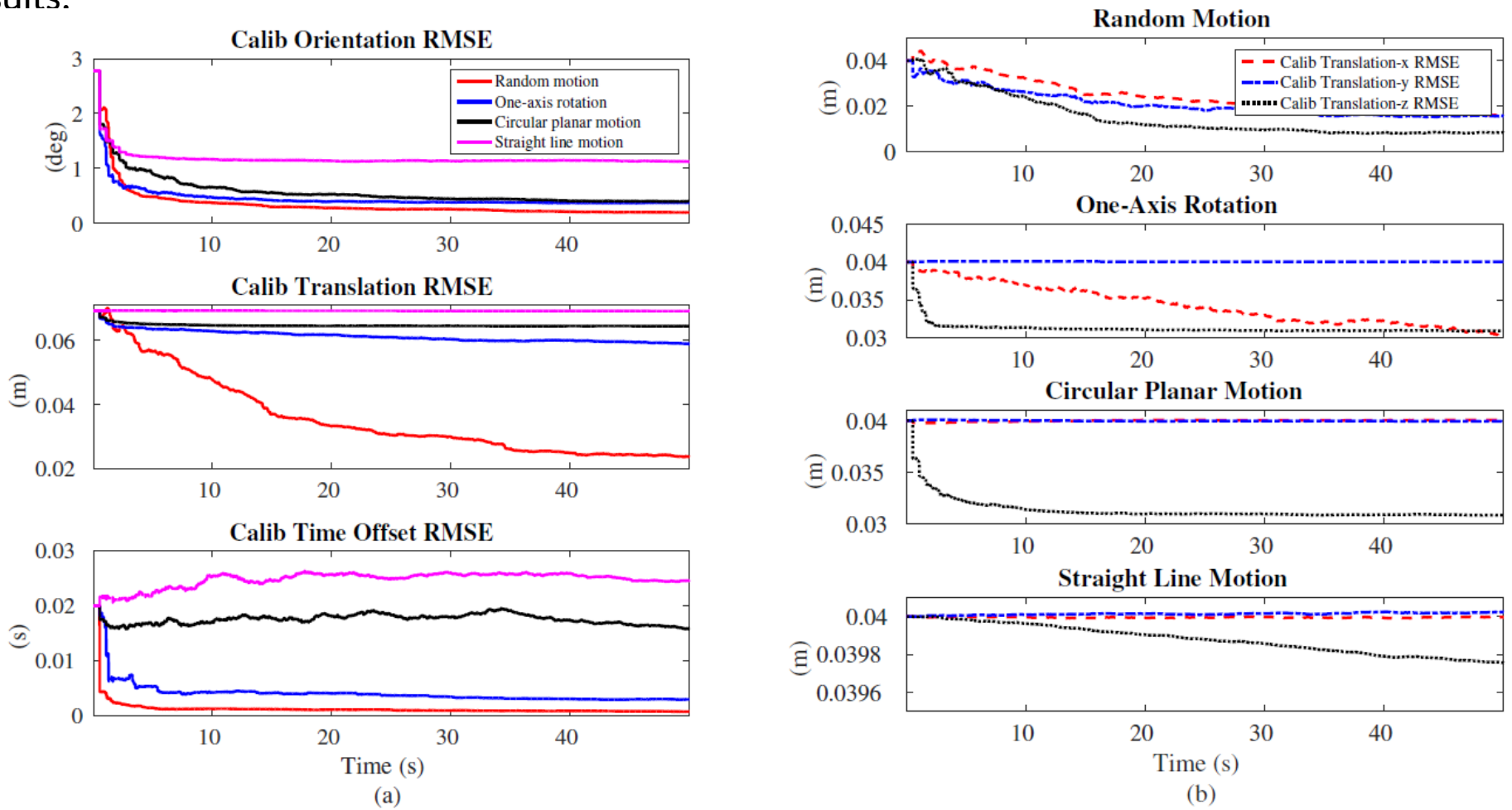

图 7： 在所有考虑的运动情况下，使用全局位置测量值 (td=0.04(sec)) 对空间和时间校准的模拟平均 RMSE

（a）时空参数的校准误差　　（b）空间校准的三轴平移误差

CONTENT OF REPORT

- **Part 1. VIO 外参 / 时间差在线标定**
- **Part 2. 退化运动的可观性分析**
- **Part 3. 结论**

结论

Conclusion：

1. 我们对具有空间和时间校准参数的线性化辅助 INS 进行了可观性分析，并表明**如果传感器平台进行一般的随机运动，则空间和时间校准参数都是可观的。**

2. 更重要的是，我们确定了在现实情况中经常遇到的**四种退化运动**，它们可能导致**在线空间和时间校准失败**。

3. 我们还研究了全局位姿测量对空间和时间校准的影响，并分析显示，**即使使用全局位姿测量，这些校准参数的退化运动仍然成立。**

4. 我们通过**在线时空校准实现了基于 MSCKF 的 VINS**，并通过蒙特卡洛模拟和典型退化运动的真实世界实验对我们的分析进行了广泛验证。将来，我们将把工作**扩展到多传感器（例如 camera， IMU 和 LiDAR）的空间和时间校准，并研究时间偏移随时间变化的情况**。

Thank you for your listening and guidance !